Cell

FOXP3 Is an X-Linked Breast Cancer Suppressor Gene and an Important Repressor of the *HER-2/ErbB2* Oncogene

Tao Zuo,[2] Lizhong Wang,[1] Carl Morrison,[3] Xing Chang,[1] Huiming Zhang,[1] Weiquan Li,[1] Yan Liu,[1] Yin Wang,[1] Xingluo Liu,[3] Michael W.Y. Chan,[2] Jin-Qing Liu,[3] Richard Love,[4] Chang-gong Liu,[2] Virginia Godfrey,[5] Rulong Shen,[3] Tim H.-M. Huang,[2] Tianyu Yang,[3] Bae Keun Park,[6] Cun-Yu Wang,[6] Pan Zheng,[1,*] and Yang Liu[1,*]

[1] Division of Immunotherapy, Section of General Surgery, Department of Surgery, Comprehensive Cancer Center, and Program of Molecular Mechanisms of Disease, University of Michigan, Ann Arbor, MI 48109, USA
[2] Program in Molecular, Cellular, and Developmental Biology and Department of Molecular Virology, Immunology, and Medical Genetics
[3] Department of Pathology
[4] Department of Internal Medicine
Ohio State University Medical Center and Comprehensive Cancer Center, Columbus, OH 43210, USA
[5] Department of Pathology, University of North Carolina, Chapel Hill, NC 27599, USA
[6] Laboratory of Molecular Signaling and Apoptosis, Department of Biologic and Materials Sciences, School of Dentistry, University of Michigan, Ann Arbor, MI 48109, USA
*Correspondence: yangl@umich.edu (Y.L.), panz@umich.edu (P.Z.)
DOI 10.1016/j.cell.2007.04.034

SUMMARY

The X-linked *Foxp3* is a member of the forkhead/winged helix transcription factor family. Germline mutations cause lethal autoimmune diseases in males. Serendipitously, we observed that female mice heterozygous for the "scurfin" mutation of the *Foxp3* gene (*Foxp3*$^{sf/+}$) developed cancer at a high rate. The majority of the cancers were mammary carcinomas in which the wild-type *Foxp3* allele was inactivated and *HER-2/ErbB2* was overexpressed. Foxp3 bound and repressed the *HER-2/ErbB2* promoter. Deletion, functionally significant somatic mutations, and downregulation of the *FOXP3* gene were commonly found in human breast cancer samples and correlated significantly with HER-2/ErbB2 overexpression, regardless of the status of *HER-2* amplification. Our data demonstrate that *FOXP3* is an X-linked breast cancer suppressor gene and an important regulator of the *HER-2/ErbB2* oncogene.

INTRODUCTION

Identification of *BRCA1* and *BRCA2* marks a key advance in understanding the genetic defects responsible for breast cancer (Miki et al., 1994; Wooster et al., 1995). Several other genes, such as *TP53*, *PIK3CA*, and *PTEN*, have also been implicated in familial and sporadic cancers (Samuels et al., 2004; Wooster and Weber, 2003). However, the genetic defects for breast cancer have yet to be fully elucidated. There is an important distinction between autosomal and X-linked genes, as many genes in the latter category are subject to X inactivation, making it easier to fulfill Knudson's two-hit theory (Knudson, 1971). As such, X-linked tumor suppressor genes can potentially be more important, as LOH or mutation of a single allele can in effect functionally silence the gene (Spatz et al., 2004). However, essentially all tumor suppressor genes are autosomal (Spatz et al., 2004), although tantalizing evidence concerning abnormalities in the X chromosome, including LOH, skewed inactivation, and selective loss, has been reported in breast cancer samples (Kristiansen et al., 2005; Piao and Malkhosyan, 2002; Richardson et al., 2006; Roncuzzi et al., 2002).

HER-2/Neu/ErbB2 is one of the first oncogenes to be identified (Schechter et al., 1984) and has been demonstrated to be expressed in a large proportion of cancer cells (Garcia de Palazzo et al., 1993). The level of HER-2/NEU is an important prognostic marker (Slamon et al., 1987). Anti-HER-2/NEU antibody Herceptin has emerged as an important therapeutic for patients with overexpressed HER-2/NEU on cancer tissues (Slamon et al., 2001). Given the clinical and therapeutic significance of *Her-2/Neu/ErbB2* overexpression, it is important to identify the molecular mechanisms responsible for the overexpression. A well-established mechanism responsible for HER-2 overexpression in human cancer is gene amplification (Slamon et al., 1987). However, it is unclear whether gene amplification alone is sufficient to cause HER-2 overexpression. Moreover, a significant proportion of human cancers with moderate overexpression of HER-2 does not show gene amplification (Bofin et al., 2004; Jimenez

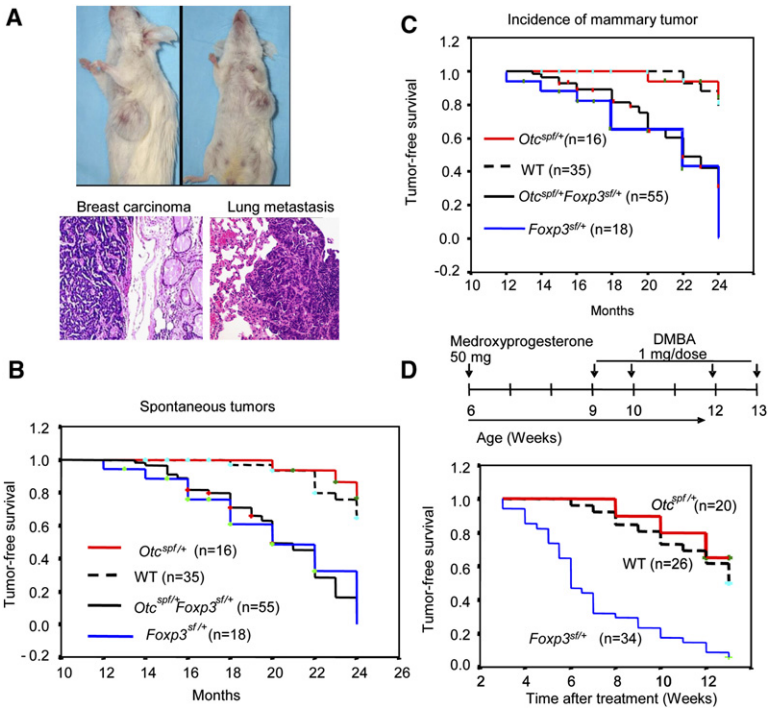

Figure 1. Increased Susceptibility to Breast Cancer in Mice Heterozygous for *Foxp3^sf^*

(A) Representative breast cancers developed in female *Foxp3^sf/+^Otc^spf/+^* mice. The top panel shows the gross anatomy, while the lower panel shows the histology of local and metastatic lesions of a breast cancer. (B) Cancer-free survival analysis of *Foxp3^sf/+^*, *Foxp3^sf/+^Otc^spf/+^*, *Otc^spf/+^*, and WT littermates. Mice were sacrificed when moribund to identify the tissue origins of cancers. *Foxp3^sf/+^* versus WT, $p < 0.0001$; *Foxp3^sf/+^* versus *Otc^spf/+^*, $p = 0.0003$; *Foxp3^sf/+^* versus *Foxp3^sf/+^Otc^spf/+^*, $p = 0.9526$; *Foxp3^sf/+^Otc^spf/+^* versus WT, $p = 0.0001$; *Foxp3^sf/+^Otc^spf/+^* versus Otc^spf/+^, $p = 0.0001$; *Otc^spf/+^* versus WT, $p = 0.4164$.

(C) As in (B), except that only incidences of mammary tumors were included. *Foxp3^sf/+^* versus WT, $p = 0.00015$; *Foxp3^sf/+^Otc^spf/+^* versus WT, $p = 0.00011$.

(D) Increased susceptibility of *Foxp3^sf/+^* mice to carcinogen DMBA and progesterone. The diagram on top depicts experimental protocol, while survival analysis is shown in the bottom panel. *Foxp3^sf/+^* versus WT, $p < 0.0001$; *Foxp3^sf/+^Otc^spf/+^* versus Otc^spf/+^, $p = 0.0005$; *Otc^spf/+^* versus WT, $p = 0.8157$. In (B) and (C), those mice that were observed for only part of the duration were incorporated as censored samples and were marked with a cross in the Kaplan-Meier survival curves. The p values in (B) and (C) were derived from log-rank tests.

et al., 2000; Todorovic-Rakovic et al., 2005). It is therefore of great interest to identify regulators for *HER-2* expression in breast cancer. In this context, Xing et al. (2000) reported that DNA-binding protein PEA3 specifically targets a DNA sequence on the *HER-2/neu* promoter and downregulates the promoter activity. It is less clear, however, whether genetic lesions of PEA3 can cause HER-2 overexpression.

Foxp3 was identified during position cloning of *Scurfin*, a gene responsible for X-linked autoimmune diseases in mice and humans (immune dysregulation, polyendopathy, enterophathy, X-linked, IPEX) (Bennett et al., 2001; Brunkow et al., 2001; Chatila et al., 2000; Wildin et al., 2001). Serendipitously, we observed a high rate of spontaneous mammary cancer. Our systemic analyses reported herein demonstrate that the *Foxp3* gene is a mammary tumor suppressor in mice and humans. Moreover, *Foxp3* represses the transcription of the *HER-2/ErbB2* gene via interaction with forkhead DNA-binding motifs in the *ErbB2* promoter.

RESULTS

Spontaneous and Carcinogen-Induced Mammary Cancer in *Foxp3^sf/+^* Female Mice

The mutant BALB/c mice we used for the initial study carried mutations in two closely linked X chromosome genes, *Foxp3^sf^* and *Otc^spf^*. During the course of the study, a spontaneous segregation of *Otc^spf^* allowed us to obtain a BALB/c *Otc^spf/+^* strain. Meanwhile, we obtained an independent line of Scurfy mice that had never been crossed to the *Spf* mutant mice and we backcrossed the *Scurfy* mutant allele (*Foxp3^sf^*) for more than 12 generations into the BALB/c background (Chang et al., 2005). Female mice with only one copy of the *Foxp3* gene survived to adulthood and appeared normal within the first year of life (Godfrey et al., 1991) with normal T cell function (Fontenot et al., 2003, 2005; Godfrey et al., 1994). Our extended observations of the retired breeders for up to two years revealed that close to 90% of the *Foxp3^sf/+^Otc^spf/+^* and *Foxp3^sf/+^* mice spontaneously developed malignant tumors. Cancer incidences in the littermate controls and a line of congenic mice with a mutation in *Otc* but not *Foxp3* were comparable with each other (Figures 1A and 1B). About 60% of the tumors were mammary carcinomas (Figures 1A and 1C), although other tumors, such as lymphoma, hepatoma, and sarcoma were observed. Histological analyses revealed lung metastasis (Figure 1A; lower panels, based on expression of ER and/or PR, data not shown) in about 40% of the mice with mammary cancer. More than a third of the tumor-bearing mice had multiple lesions in the mammary glands. Most, although not all, mammary carcinomas expressed the estrogen receptor (ER^+, 14/18) and progesterone receptor (PR^+, 12/18).

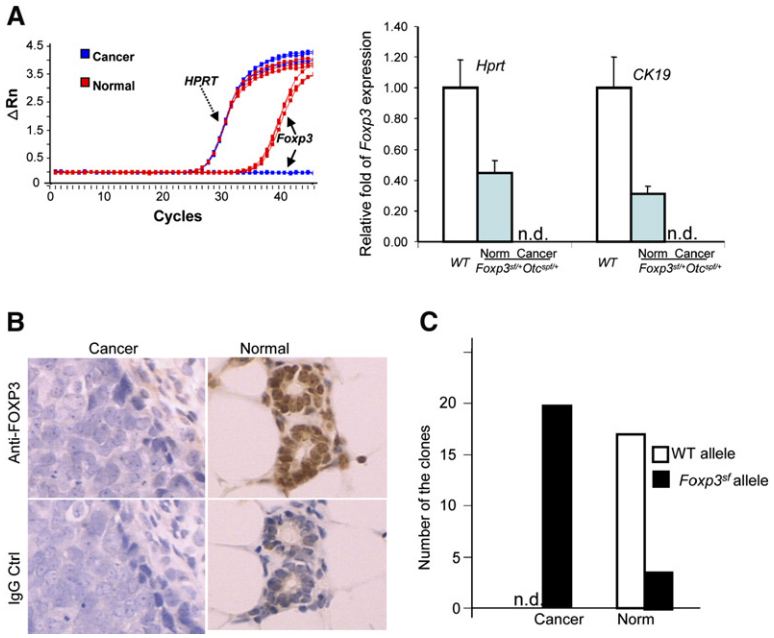

Figure 2. Inactivation of the WT *Foxp3* Allele in Mammary Cancer Cells

(A) Defective *Foxp3* expression in breast cancer. RNA extracted from the cells isolated by laser-capture microdissection was subjected to quantitative real-time RT-PCR using primers specific for *Foxp3, Hprt*, and *CK19*. In the left panel, fluorescence intensity (ΔRn) was plotted versus cycle number. Mean and standard deviation (SD) from three individual mice per group are presented in the right panel ($p < 0.0001$, one-way ANOVA test when either internal standard was used).

(B) Immunohistochemical staining of normal mammary glands and adenocarcinomas from a $Foxp3^{sf/+}Otc^{spf/+}$ mouse using rabbit anti-FOXP3 polyclonal antibody and normal rabbit IgG as the control.

(C) Specific silencing of the WT allele in breast cancer cells. *Foxp3* transcripts were amplified from microdissected breast cancers or normal breast epithelium by two rounds of anchored PCR and were cloned into the TOPO vector and sequenced. The number of clones with sequences of WT or mutant alleles in the breast cancer and normal epithelium is presented. A total of 20 clones were sequenced from each group. Data shown are from pooled samples that lack *CD3* transcripts. n.d., not detectable.

In order to focus on mammary cancer, we treated the mice with a carcinogen, 7,12-dimethylbenz [a] anthracene (DMBA), in conjunction with progesterone. Mice heterozygous for $Foxp3^{sf}$, but not those heterozygous for Otc^{spf}, showed substantially increased susceptibility to mammary cancer, as revealed by earlier onset and increased incidence (Figure 1D) and multiplicity (data not shown) of the breast tumors. These data demonstrate that a mutation of *Foxp3*, but not *Otc*, results in a major increase in susceptibility to mammary carcinoma.

Foxp3 Expression in Normal and Cancerous Mammary Tissues

Since expression of *Foxp3* has not been reported in mammary tissue, we isolated normal and cancerous cells by laser-capture microdissection (Figure S1A) and compared expression of *Foxp3* and *Otc* by real-time RT-PCR and histochemistry. The complete absence of the *cd3* transcripts (Figure S1B) indicated that the microdissected samples were devoid of T cells, the main cell types known to express *Foxp3* (Fontenot et al., 2005). A representative profile and summarized data of *Foxp3* expression in $Foxp3^{sf/+}Otc^{spf/+}$ mice and age-matched *wild-type* (*WT*) control mice are shown in Figure 2A. *Foxp3* mRNA was detected in normal mammary epithelium from both the WT and $Foxp3^{sf/+}Otc^{spf/+}$ mice, but not in mammary cancer cells from the same $Foxp3^{sf/+}Otc^{spf/+}$ mice. Immunohistochemical staining (Figure 2B) confirmed the loss of expression of *Foxp3* in the mammary carcinoma generated from the $Foxp3^{sf/+}Otc^{spf/+}$ mice.

Foxp3 is an X-linked gene that is subject to X-chromosomal inactivation (Fontenot et al., 2005). We carried out an anchored RT-PCR and cloned the low levels of *Foxp3* mRNA in the breast tissues. We sequenced the cDNA clones from pooled samples after ruling out potential T cell contamination (based on a lack of T cell specific *cd3* transcripts; Figure S1B). As shown in Figure 2C, 100% of the *Foxp3* transcripts in the cancerous tissues were from the mutant alleles, which indicate that the wild-type allele was silenced in the tumor cells. In contrast, the transcripts from the mutant allele constituted 15% of the transcripts in the normal mammary samples from the same mice. Thus, the expression pattern of *Foxp3* fulfills another criterion for a tumor suppressor gene.

FOXP3 Is a Repressor of *ErbB2* Transcription

Our characterization of the mammary tumors in the mutant mice revealed widespread upregulation of ErbB2, in contrast to those rare tumors from WT mice, as shown in Figure 3A and Table S1. Using real-time RT-PCR, 8- to 12-fold more *ErbB2* mRNA was found in the cancer cells than in normal epithelium (Figure 3A). There was also more *ErbB2* mRNA in the $Foxp3^{sf/+spf/+}$ epithelium than in that of the *WT* female mice (Figure 3A), which indicates a potential gene dosage effect of *Foxp3* on the regulation of *ErbB2* expression in vivo. Transfection of the TSA cell line with *Foxp3* cDNA repressed *ErbB2* levels on the TSA cell line (Figure 3B).

Analysis of the 5′ sequence of the *ErbB2* gene revealed multiple binding motifs for the forkhead domain (Figure 3C). To test whether Foxp3 interacts with the *ErbB2* promoter, we used anti-V5 antibody to precipitate sonicated chromatin from the TSA cells transfected with the Foxp3-V5 cDNA and used real-time PCR to quantitate

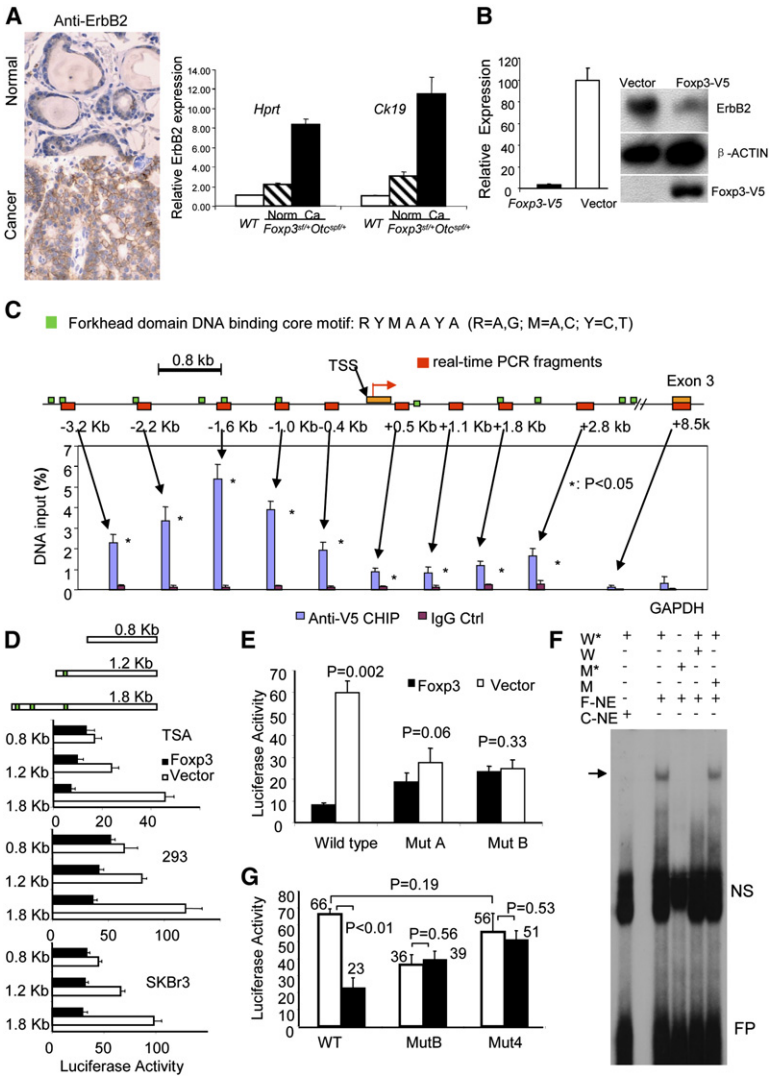

Figure 3. *Foxp3* Represses the Expression of *ErbB2*

(A) Overexpression of *ErbB2* in mouse mammary cancers. The left panels show immunohistochemical staining of a noncancerous mammary gland and an adjacent adenocarcinoma from a $Foxp3^{sf/+}Otc^{spf/+}$ mouse using anti-ErbB2 antibody. The right panel shows relative expression levels of *ErbB2* in normal mammary epithelium of *WT* and $Foxp3^{sf/+}Otc^{spf/+}$ mice and of cancer tissues from $Foxp3^{sf/+}Otc^{spf/+}$ mice as revealed by real-time RT-PCR of LCM samples. Data shown are means and SD. The expression of *ErbB2* was normalized against either *Hprt* or *CK19*. Highly significant differences were observed between cancerous and normal tissue ($p < 0.001$, ANOVA test when either internal standards were used).

(B) Transfection of *Foxp3-V5* into TSA cells repressed expression of the *ErbB2* locus. The left panel shows mRNA levels as measured by real-time PCR. Data shown are means and SD of triplicates. The right panel shows the protein levels by western blot of the cell lysates using anti-ErbB2 antibody. The amount of actin-β was used as loading control, while the amount of transfected Foxp3-V5 was measured by western blot using anti-V5 antibodies.

(C) Binding of the Foxp3-V5 fusion protein to the promoter region of the *ErbB2* gene. Top panel is a diagram of the 5′ region of the *ErbB2* gene, including the promoter, exon 1, intron 1, and exon 3. The forkhead-binding motifs are illustrated with small green bars, while the regions surveyed by real-time PCR are marked in red bars. The lower panel shows the amount of DNA precipitated by either control IgG or anti-V5 mAb expressed as percentage of the total input genomic DNA. Data shown are means and standard deviation (SD) of triplicates. This experiment has been repeated twice with similar results.

(D) *Foxp3*-mediated repression of the *ErbB2* promotor requires forkhead-binding motifs as evaluated by dual-luciferase reporter assay. The promoter regions differed in the number of forkhead-binding motifs, as illustrated in the diagram on the left. Three different cell lines were transfected with either vector control or *Foxp3* (1 μg/well) in conjunction with the luciferase reporter driven by different 5′ promoter regions of the *ErbB2* gene (0.6 μg/well). pRL-TK was used as internal control. The luciferase activity from the cells transfected with the pGL2-basic vector was arbitrarily defined as 1.0. Data shown are means and SD of triplicates and have been repeated at least three times.

(E) Site-directed mutagenesis of one of two conserved regions with multiple forkhead-binding motifs in the *ErbB2/HER-2* promoter prevented repression of the *ErbB2* promoter by *Foxp3*. The two binding sites, as illustrated in Figure S2, were deleted individually (deleted DNA sequence, Mut A: AAATCTGGGATCATTTA; Mut B: TTTGAATTTCAGATAAA). Mutations of either site prevented *FOXP3*-mediated suppression. The promoter activity was measured and normalized as detailed in (D), except that the amount of promoter DNA was 0.4 μg/sample. The promoter activities of the vector groups were artificially defined as 1.0. Data shown are means and SD of triplicates. This experiment has been repeated twice with similar results.

(F) Foxp3-mediated binding to specific *cis* elements in the *ErbB2* promoter. Nuclear extracts from the F*oxp3-V5*- (F-NE) or vector-transfected control (C-NE) TSA cells were preincubated with ^{32}P-labeled WT (*W) or mutant probes (*M) in the presence of an unlabeled WT (W) or mutant probe (M). The mixtures were analyzed by PAGE. NS, nonspecific; FP, free probe. The specific Foxp3-shifted band is marked by an arrow. Data shown have been repeated three times.

(G) Mutation of forkhead binding motifs (Mut 4) abrogated FOXP3-mediated repression, but not basal promoter activity. This is as in (E), except that WT, Mut B, and Mut 4 (mutations that inactivate the Foxp3 binding as detailed in [F]) of the *ErbB2* promoters were used. This experiment has been repeated twice with similar results. The differences were compared by student t tests with p value provided. Data shown are means and SD of triplicates.

the amounts of the specific *ErbB2* promoter region precipitated by the anti-V5 antibodies in comparison to those that bound to mouse IgG control. As shown in Figure 3C, the anti-V5 antibodies pulled down significantly higher amounts of *ErbB2* promoter DNA than the IgG control, with the highest signal around 1.6 kb 5′ of the transcription starting site.

To test whether the binding correlated with the suppression by Foxp3, we produced luciferase reporter using the 1.8, 1.2, and 0.8 Kb upstream of the *ErbB2* TSS and tested

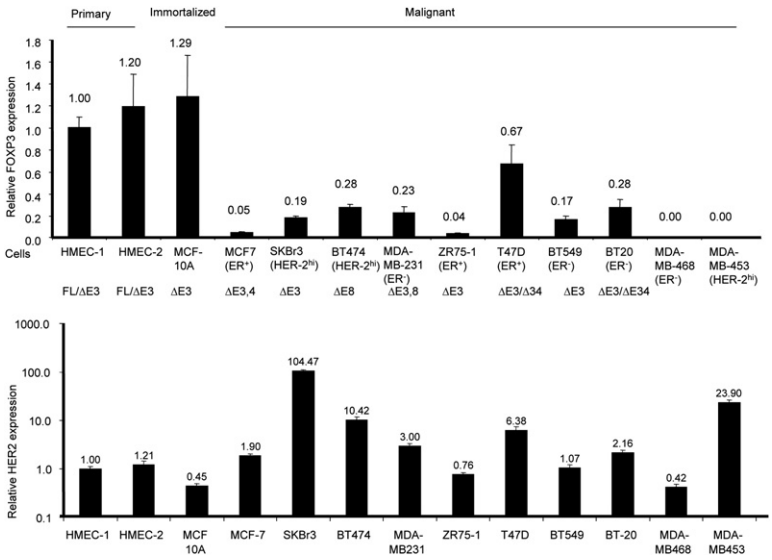

Figure 4. Characterization of *FOXP3* Transcripts in Primary, Immortalized, and Malignant Mammary Epithelial Cells

Relative levels and isoforms of *FOXP3* (the upper panel) and *HER-2* (the lower panel) mRNA. After normalizing against endogenous *GAPDH*, the amounts of transcripts were compared to those found in HMEC-1, which was arbitrarily defined as 1.0. Data shown are means and SD of triplicates. This experiment has been repeated twice with similar results. The reported ER status and the isoforms of the *FOXP3* transcripts detected are indicated. To characterize the isoforms, *FOXP3* mRNA was amplified by two rounds of anchored PCR using primers annealing to exons 1 and 12. The bulk PCR products were sequenced only if one species was found in agarose electrophoresis. When more than one species was observed, the PCR products were cloned and multiple clones were sequenced until all of the species observed in the agarose gel were identified.

the ability of Foxp3 to repress *ErbB2* promoter activity. In three separate cell lines, we observed that the region with the strongest ChIP signal was required for optimal-repression by Foxp3 (Figure 3D). Furthermore, we deleted two potential Foxp3 binding sites based on intensity of ChIP signal, abundance of consensus binding sites, and conservation between mouse and human (Figure S2) by site-directed mutagenesis and measured the effect on Foxp3-mediated repression. As shown in Figure 3E, deletion of either binding site substantially increased the *ErbB2* promoter activity in the presence of Foxp3 and thus alleviated Foxp3-mediated repression.

Since the region deleted in Mut B is 100% conserved between mouse and man and since this deletion completely wiped out repression, we used an electrophoretic mobility shift assay (EMSA) to determine whether the forkhead DNA-binding motifs in region B bound to Foxp3. As shown in Figure 3F, the nuclear extracts from the Foxp3-expressing cells specifically retarded migration of the WT but not mutant ^{32}P-labeled probes compared with control cells. While mutant cold probes did not affect Foxp3-binding activities, WT cold probes significantly diminished them, establishing that the binding of these complexes is specific to forkhead DNA-binding motifs. We therefore carried out site-directed mutagenesis to replace the 12 nucleotides (Mut C) within the *ErbB2* promoter and compared the promoter activity and Foxp3-repression by luciferase assays. While the wild-type promoter was repressed by Foxp3, no repression by Foxp3 was observed when the mutant promoter was used. Moreover, in contrast to the deletional Mut B, the mutations had no impact on the basal activity of the *ErbB2* promoter (Figure 3G). Taken together, our new data make a compelling case that Foxp3 represses the *ErbB2* promoter via specific forkhead-binding motifs.

FOXP3 Defects in Human Breast Cancer

We analyzed the levels and isoforms of the *FOXP3* transcripts in a panel of normal human mammary epithelial cells (HMEC), an immortalized but nonmalignant cell line (MCF-10A), and ten malignant breast cancer cell lines differing in ER/PR and HER-2 status. Early passage of HMEC with no methylation in the CpG island of the *P16* promoter (Figure S3) was used to avoid effects associated with *P16* inactivation in postsenescence HMEC cultures (Romanov et al., 2001). As shown in Figure 4A, similar levels of *FOXP3* transcripts were observed in two independent isolates of HMEC and in the immortalized cell line MCF-10A. Each of the ten tumor cell lines had a different degree of reduction in *FOXP3* mRNA levels in comparison to HMEC and MCF-10A. Among them, two were completely devoid of FOXP3 mRNA, while the others had a 1.5- to 20-fold reduction. We then used anchored primers spanning exons 1–12 to amplify the FOXP3 transcripts, and then we sequenced the PCR products. As shown in Figure 4, none of the tumor cell lines expressed full-length *FOXP3* transcripts. The HMEC expressed the same two isoforms as observed in the T cells, while MCF-10A expressed the exon 3-lacking isoforms. The same isoform was also found in four tumor cell lines at much lower levels. In addition, three tumor cell lines expressed an isoform lacking both exons 3 and 4. The alternative splicing resulted in a frameshift beginning at codon 70 and an early termination at codon 172. Furthermore, two tumor cell lines expressed a *FOXP3* isoform lacking exons 3 and/or 8. Exon 8 encodes the leucine-zipper domain that is frequently mutated in IPEX patients (Ziegler, 2006). Thus, *FOXP3* is abnormal in breast cancer cell lines. Consistent with a role for *FOXP3* in repressing *HER-2* expression, the majority of the breast cancer cell lines had higher levels of HER-2 in comparison to normal HMEC (Figure 4, lower panel). However, additional changes are also likely

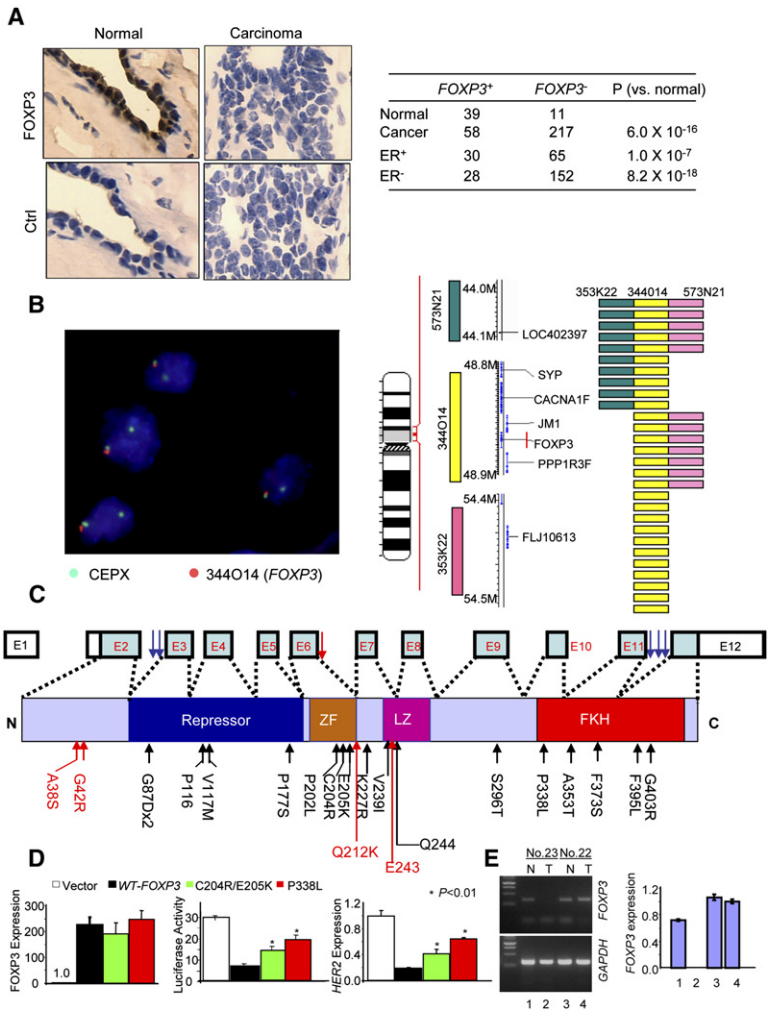

Figure 5. *FOXP3* Defects in Human Breast Cancer

(A) Downregulation of the FOXP3 protein among human breast cancer cells. Photographs in the top panels show anti-FOXP3 staining of normal and carcinoma tissues from the same patient, with specificity control shown at the bottom. The number and percentage of FOXP3 positive tissues are shown in the right panel. Samples with nuclear staining by the anti-Foxp3 antibody were scored as positive.

(B) Deletion of the *FOXP3* locus in breast cancer cells. Breast cancer tissue microarray samples were analyzed by FISH using three BAC clone probes surrounding a 10 MB region in Xp11.2. A typical FISH for the CEPX (green) and *FOXP3* (orange) probes is shown on the left, while the genomic structure of the X chromosome and probe positions are illustrated in the middle panel. A total of 238 samples were analyzed for all probes, with 223 samples providing definitive FISH data. Twenty-eight of the two hundred and twenty-three samples showed deletions as detected by at least one of the three probes. The positions of the deletions in the 28 samples are summarized in the right panel.

(C) Somatic mutation of the *FOXP3* gene in breast cancer samples: summary of sequencing data from 65 cases, including 50 formalin-fixed samples and 15 frozen samples. Genomic DNA was isolated from matched normal and cancerous tissues from the same patients and amplified with primers for individual exons and intron-exon boundary regions. Somatic mutations were identified by comparing sequences from normal and cancerous samples from the same patients. The data are from either bulk sequencing of PCR products or from the sequencing of 5–10 clones from PCR products. Only those mutations that were observed in multiple clones were scored. Mutations identified from 50 cases of formalin-fixed samples are marked in black, while those identified from 15 cases of frozen tissue samples are marked in red.

(D) *FOXP3* mutations reduced its repressor activity for the *HER-2* promoter in the SKBr-3 cell line. The left panel shows expression of mutant cDNA. The middle panel shows luciferase activity, while the right panel shows the levels of *HER-2* transcripts. The difference between WT and 318 P > L and that between WT and 204C > R205E > K are highly significant ($p < 0.01$). Data shown are means and SD of triplicates and representative of at least two to three independent experiments.

(E) A breast cancer sample with a somatic mutation in intron 6 (case 23) had an inactivated *FOXP3* locus. Normal mammary epithelial (N) and tumor (T) cells were isolated by LCM. The *FOXP3* transcripts were determined either by PCR using primers spanning exons 5–8 to detect alternatively spliced products or by real-time PCR using primers spanning exons 10–12. The upper and middle panels show photographs of PCR products of *FOXP3* or *GAPDH* loci, while the right panel shows the relative level of *FOXP3* transcripts as determined by real-time PCR. Neither assay detected any *FOXP3* transcripts in the tumor of case no. 23. Substantial amounts of *FOXP3* transcripts were detected in normal samples and tumors in case no. 22 (with a synonymous mutation in exon 7), which was artificially defined as 1.0. Data shown are means and SD of triplicates. This experiment has been repeated twice with similar results.

required for *HER-2* overexpression, as three cell lines did not overexpress *HER-2* even though the *FOXP3* transcripts were greatly reduced.

We took three approaches to determine whether the findings in the mutant mice and human breast cancer cell lines are relevant to the pathogenesis of human breast cancer. First, we used immunohistochemistry to determine expression of FOXP3 in normal versus cancerous tissue. As shown in Figure 5A, while about 80% of the normal breast samples expressed FOXP3 in the nuclei of the epithelial cells, only about 20% of the cancerous tissue showed nuclear staining. Second, we used fluorescence in situ hybridization (FISH) to determine whether the *FOXP3* gene was deleted in the breast cancer samples. The minimal common region of deletion was identified using flanking p-telomeric and centromeric clones. Out of 223 informative samples, we observed 28 cases (12.6%) with deletions in any of the three loci. Interestingly, deletion of the *FOXP3* locus was found in all of the 28 cases (Figure 5B and Table S2). These data suggest

that *FOXP3* is likely within the minimal region of deletion in the Xp11 region studied. Although all deletions were heterozygous, the FOXP3 protein was undetectable in 26 out of 28 cases. Thus, it appears that for the majority of the breast cancer samples, LOH alone was sufficient to inactivate the locus, perhaps due to X-chromosomal inactivation. The two cases with both deletion and FOXP3 expression had X polysomy with three and four X chromosomes, respectively (Table S2). Thirdly, we isolated DNA from matched normal and cancerous tissues (50 cases with formalin-fixed samples and 15 cases of frozen samples) from patients with invasive ductal carcinoma and amplified all 11 coding exons and intron-exon boundary regions by PCR. Two independent PCR products were sequenced in order to confirm the mutations. Unless the bulk sequencing data were unambiguous (Figures S4A and S4C), the PCR products were cloned, and five to ten independent clones from each reaction were sequenced (Figure S4B). Among the formalin fixed samples, we only used the cases in which the normal tissue samples gave unambiguous sequencing data that matched the wild-type *FOXP3* sequence. When the cancerous tissues were compared with normal tissues from the same patient, 36% (18 out of 50 formalin-fixed samples and 5 out of 15 frozen samples) showed somatic mutations (Table S3). Loss of the wild-type allele was found in 6 out of 23 cases (38%) of cancer samples with somatic *FOXP3* mutations (see Figure S4C for an example). The other cases had heterozygous mutations (Figure S4A). Eighteen mutations resulted in the replacement of amino acids. Most are likely to be critical for FOXP3 function, as judged from the pattern of mutation in IPEX patients (Ziegler, 2006) or in the conserved zinc finger domain that has so far not been implicated (Figure 5C).

Although most samples had a single mutation of the *FOXP3* gene, we did observe two cases with multiple mutations. In the first sample (Figure S4B; case 3 in Table S3), the two mutations occurred in consecutive codons, resulting in two nonconservative replacements of amino acid residues. Clonal analysis revealed that both mutations occurred in the same clone (Figure S4B). In the second sample (Table S3; case 16), three mutations occurred in intron 11. Since this case lacked a WT allele (Figure S4D), it is likely that all of the mutations occurred in the same allele. The possibility of a mismatch in the cancer and normal samples was ruled out by comparing the normal and cancer samples for polymorphism of two unrelated genes (data not shown).

To directly test whether *FOXP3* mutations affect the repressor activity for the *HER-2* gene, we chose two representative somatic *FOXP3* mutants isolated in the cancer cells and tested their repressor activity for the *HER-2* promoter. One mutation (338P > L) resided in the signature forkhead domain, which is often mutated in the IPEX patient, while the other double mutation (*204C > R205E > K*) was from the zinc finger domain that has not been implicated in IPEX patients. As shown in Figure 5E, both mutations significantly reduced the repressor activity of FOXP3. The reduced repression of the *HER-2* promoter correlates with a significantly reduced inhibition of *HER-2* mRNA (Figure 5D).

Four cases had mutations in introns that may potentially affect RNA splicing. We used laser-guided microdissection to isolate normal and cancerous epithelial cells from one case with a mutation in intron 6 (case 23; Table S3). RNA was isolated and tested for the potential effects of the mutation on RNA splicing (using primers on exons 5 and 8) and total *FOXP3* transcript, as quantitated by real-time PCR using primers spanning exons 10–12. Tissues from another patient with a mutation in exon 7 were used as control. As show in Figure 5E's left panel, primers spanning exons 5 and 8 failed to detect *FOXP3* mRNA from the cancerous tissue of case no. 23. Furthermore, primers spanning exons 10–12 also failed to detect any *FOXP3* transcripts. Substantial levels were detected in the normal epithelial cells of the same patients as well as in normal and cancerous tissues from case no. 22. Since the wild-type allele had been lost in the cancer cells of case no. 23, it is likely that the mutation in intron 6 inactivated *FOXP3.* With an intron of 944 nucleotides, a mutation that prevented splicing of intron 6 would cause premature-termination codon-mediated RNA decay, which is operative in the *FOXP3* gene (Chatila et al., 2000).

FOXP3 Defects and HER-2 Overexpression

To demonstrate a role for *FOXP3* defect in *HER-2* overexpression, we first silenced the *FOXP3* gene in early passage of primary HMEC (Supplemental Fig. S3) using a lentiviral vector expressing *FOXP3* siRNA. As shown in Figure 6A, the *FOXP3* siRNA reduced *FOXP3* expression by more than 100-fold while increasing *HER-2* mRNA by 7-fold. A corresponding increase in cell surface HER-2 was also observed (Figure 6B). These results implicate *FOXP3* as a repressor of *HER-2* in human breast epithelial cells.

Second, since a major mechanism for HER-2 upregulation in breast cancer is gene amplification (Kallioniemi et al., 1992), an intriguing issue is whether *FOXP3* is capable of repressing HER-2 in cancer cells with an amplified HER-2 gene. We produced a Tet-off line of BT474, a breast cancer cell line known to have *HER-2* gene amplification (Kallioniemi et al., 1992), and transiently transfected it with a *pBI-EGFP-FOXP3*- vector. After drug selection, the cells were cultured either in the presence or absence of doxycycline. While the cells cultured with doxycycline did not express FOXP3 (data not shown), removal of doxycycline resulted in induction of FOXP3 in a significant fraction of the cancer cells, which allowed us to compare HER-2 levels in the $FOXP3^+$ and $FOXP3^-$ cells in the same culture by flow cytometry. As shown in Figure 6C, $FOXP3^-$ cells had about a 5- to 10-fold higher level of the HER-2 protein on the cell surface in comparison to the $FOXP3^+$ cells.

Thirdly, we compared the expression of FOXP3 with HER-2 expression in breast cancer tissues. As shown in

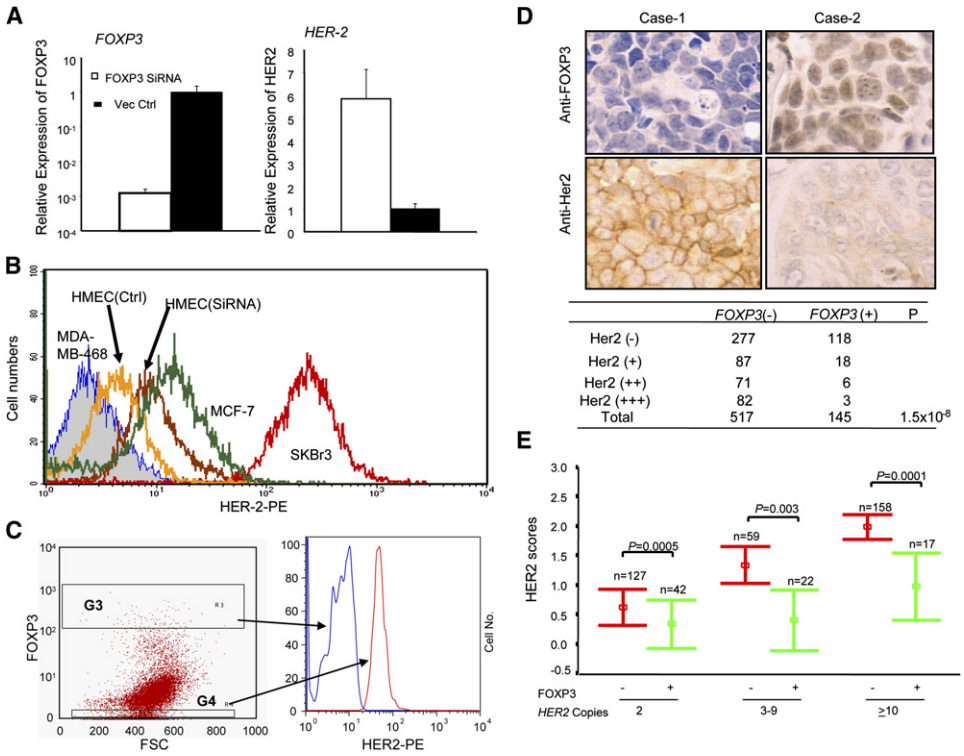

Figure 6. *FOXP3* Is an Important *HER-2* Repressor

(A) Silencing of FOXP3 resulted in the upregulation of HER-2 in primary human mammary epithelial cells (HMEC). Early passage of HMEC were transduced with lentiviral vector for either control sequence or *FOXP3* siRNA. The untransfected cells were removed by selection with blasticidin. At 1 week after transduction, the levels of the *FOXP3* and *HER-2* transcripts were quantitated by real-time PCR. Data shown are mean and standard error of the mean of relative levels of transcripts (with that in the vector-transduced cells defined as 1.0) and represent those of three independent experiments.

(B) Flow cytometry data showing the effect of FOXP3 silencing on HMEC surface HER-2 levels. HER-2-negative MDA-MB468, HER-2^{lo} MCF-7 and HER-2^{hi} SKBr3 cell lines were included for comparison.

(C) In the Tet-off inducible *FOXP3*-expressing BT474, *FOXP3* repressed *HER-2*. BT474 cells were first transfected with pTet-Off vector. The transfectants were selected by both blasticidin and G418 in doxycycline-containing medium. The drug-resistant cells were cultured in the absence of doxycycline for 5 days to induce FOXP3. The cells were stained for FOXP3 and HER-2 proteins by flow cytometry. Data shown are histograms depicting HER-2 levels among the gated FOXP3^{hi} and FOXP3^{-} cells based on reactivity to the anti-Foxp3 antibody and are representative of those from two independent experiments.

(D) Inverse correlation between FOXP3 expression (the top panel) and that of the HER-2 (middle panel) among the human breast cancer samples. Tissue microassay samples were stained with either anti-FOXP3 antibodies or anti-HER-2 antibodies and were scored by two different pathologists in a double-blind fashion. FOXP3 staining was scored by nuclear staining with affinity-purified anti-FOXP3 antibodies. A summary of 517 FOXP3^{+} and 145 FOXP3^{-} samples is shown in the bottom panel.

(E) Inverse correlations between FOXP3 expression and HER-2 scores in cells with or without *HER-2* amplification. The *HER-2* gene-copy number was determined by FISH, while nuclear expression of FOXP3 was determined by immunohistochemistry. Data shown are mean and SD of HER-2 scores of 425 cases of breast cancers grouped by *HER-2* copy number. P values were generated by the Mann-Whitney test.

Figure 6D, downregulation of FOXP3 was strongly associated with the overexpression of HER-2, which supports a role for *FOXP3* inactivation in *HER-2* overexpression in breast cancer. Nevertheless, since many of the FOXP3^{-} cells remained HER-2^{-}, it is likely that disregulation of *FOXP3* is insufficient for *HER-2* upregulation. On the other hand, since only 3 of 82 FOXP3^{+} cancer cells expressed high levels of HER-2, *FOXP3* inactivation is likely important for *HER-2* upregulation under most circumstances.

Fourth, we divided breast cancer samples based on their *HER-2* gene copy numbers and compared the FOXP3^{+} and FOXP3^{-} cancer samples for the relative amounts of cell surface HER-2 expression. As shown in Figure 6E, in each of the gene-dose categories, FOXP3^{+} samples had reduced HER-2 scores in comparison to the FOXP3^{-} samples. These results strongly suggest a critical role for FOXP3 in repressing HER-2 expression even in the cases of *HER-2* gene amplification.

Fifth, of the 223 informative samples among the 238 that we screened for Xp11.2 deletions, those with deletions encompassing the *FOXP3* locus had significantly higher HER-2 scores compared to those without deletions ($p = 0.03$) (Table S4). Likewise, we compared the relative HER-2 scores among the 50 samples in which we had sequenced all *FOXP3* exons. As shown in Table S5, the

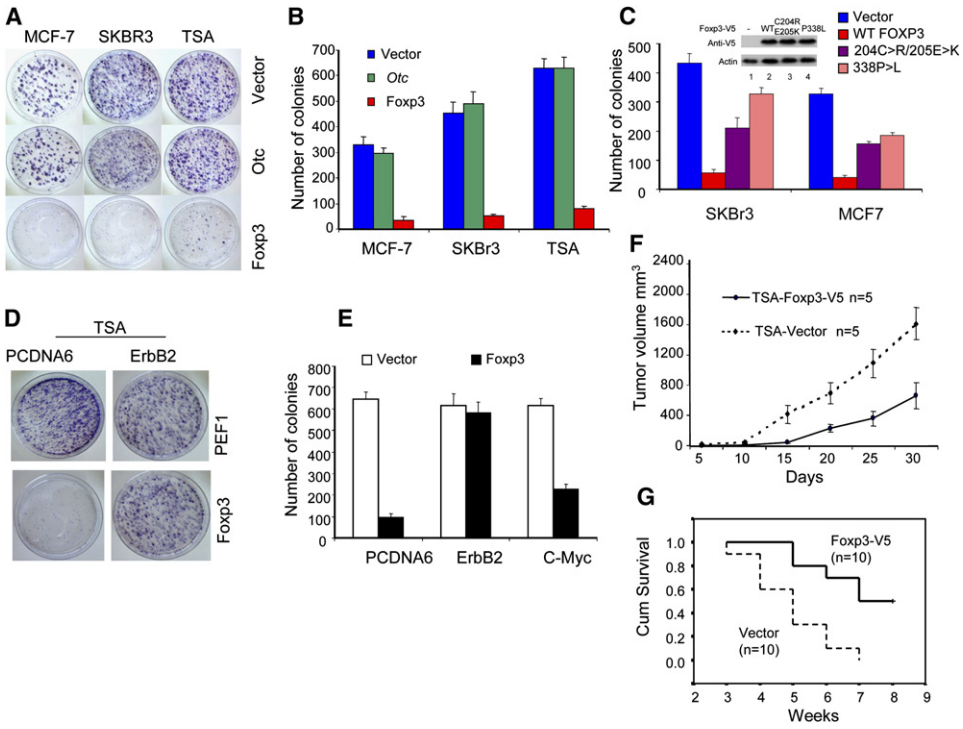

Figure 7. *Foxp3* Inhibits the Growth and Tumorigenicity of Multiple Breast Cancer Cell Lines

(A) Breast cancer cell lines MCF-7, SKBr3, and TSA were transfected with equal concentrations of vector alone (Vector), *Foxp3*, or *Otc* cDNA. After 3 weeks of G-418 selection, the drug-resistant clones were visualized by crystal violet dye.

(B) Summary of the colony numbers in three independent experiments as described in (A). Data shown are means and SD.

(C) Somatic mutations identified from breast cancer samples attenuated the growth suppression of the FOXP3. This is as in (A) and (B), except that two somatic mutants were compared with WT *FOXP3* cDNA using the two human breast cancer cell lines. Data shown are means and SD of triplicates and are representative of two independent experiments. Expression of WT and mutant proteins at 1 week after transfection is presented in the insert.

(D and E) Ectopic expression of the *ErbB2* but not the *c-Myc* cDNA abrogated *Foxp3*-mediated repression. TSA cells were transfected with either pcDNA6-blasticidin vector or *ErbB2* cDNA and selected with blasticidin for 2 weeks. Pools of blasticidin-resistant cells were supertransfected with the pEF1-G418 vector or *Foxp3* cDNA. The cells were then plated and selected with blasticidin and G418 for 3 weeks. The viable colonies were visualized after staining with the crystal violet dye. Shown in (D) are photographs of a representative plate showing abrogation of *Foxp3*-mediated suppression by *ErbB2*. Shown in (E) are the mean and SD of the colony numbers. This experiment has been repeated twice with essentially identical results.

(F) Expression of *Foxp3* reduced growth rate of tumors. Syngeneic BALB/c mice were injected with 5×10^5/mouse *Foxp3* or vector-transfected TSA cells in the flank, and the sizes of the local tumor mass were measured using a caliper. Data shown are means and SD and have been repeated once.

(G) The survival of tumor-bearing mice was monitored over a 7-week period ($p = 0.0015$, log-rank test). As in (F), except that 10^6 tumor cells/mouse were injected, and the mice were euthanized when they became moribund.

mutations in the FOXP3 gene correlated with higher levels of HER-2 ($p = 0.0083$).

Foxp3/FOXP3 Inhibits Tumorigenicity of Breast Cancer Cells

To test whether the *Foxp3* gene can suppress the growth of breast cancer cells, we transfected the empty vector or the vectors carrying either *Foxp3* (mouse or human origin) or *Otc* cDNA into three breast cancer cell lines, including mouse mammary tumor cell line TSA or human breast cancer cell lines MCF7 ($ER^+HER\text{-}2^{low}$, no *HER-2* amplification) and SKBr3 ($ER^-HER\text{-}2^{high}$ with *HER-2* amplification). The untransfected cells were removed by a selection with G418. While the vector-transfected cells grew rapidly, the *Foxp3*-transfected cell lines seldom grew into large colonies. The *Foxp3*-transfected culture had a drastic reduction in both the size and the number of the drug-resistant colonies. No effect was observed when the *Otc* cDNA was used (Figures 7A and 7B).

To test whether the somatic mutations uncovered from cancerous tissues ablated their growth inhibition, we transfected WT and two mutant Foxp3 cDNA into SKBr3 and MCF7 cell lines. As shown in Figure 7C, in both cell lines, the mutants had a greatly reduced ability to suppress tumor growth.

To test whether repression of *ErbB2* explains the tumor suppressor activity of the *Foxp3* gene in the $ErbB2^+$ cancer cell line, we transfected TSA cells with mouse CMV promoter-driven *ErbB2* cDNA cloned into the pcDNA6 vector and evaluated their susceptibility to *Foxp3*-mediated growth suppression. In this setting, the expression of *ErbB2* was resistant to *Foxp3*-mediated repression

(data not shown). If repression of endogenous *ErbB2* is critical for *Foxp3*-mediated tumor suppression, ectopic expression of *ErbB2* should alleviate the growth inhibition by *Foxp3*. As shown in Figures 7D and 7E, while the pcDNA6-vector-transfected TSA cells remained susceptible to *Foxp3*-mediated repression, the *ErbB2*-transfected TSA cells were completely resistant. In contrast, transfection of *c-Myc* barely alleviated the growth inhibition by *FOXP3* (Figure 7E). These results suggest that *Foxp3* suppresses TSA growth by repressing transcription of *ErbB2*.

We transfected TSA cells with either empty vector or V5-tagged *Foxp3* cDNA. The stable transfectant cell lines were selected by G-418. The vector and *Foxp3-V5*-transfected cell lines were injected into syngeneic BALB/c mice, which were then observed for tumor growth and mouse survival. As shown in Figure 7F, *Foxp3*-transfectants showed reduced growth in vivo. The mice that received TSA-vector cells became moribund earlier with higher incidence, while about 50% of the mice that received the *Foxp3-V5*-transfected cells survived more than 7 weeks (Figure 7G). Similarly, *Foxp3*-transfected 4T1, a mouse mammary cancer cell line with *ErbB2* overexpression, also showed reduced tumorigenicity in vivo (data not shown).

DISCUSSION

Foxp3 Is an X-Linked Mammary Tumor Suppressor Gene

Serendipitously, we observed that mice heterozygous for the *Foxp3* mutation spontaneously developed mammary cancer at a high rate. Since two independently maintained lines sharing the *Foxp3* mutation have a comparably higher incidence of mammary cancer, the *Foxp3* mutation is likely responsible for the increased rate of breast cancer. Unlike essentially all cancer suppressor genes identified to date, *Foxp3* is X-linked and inactive in cells in which the WT allele was silenced by X inactivation. This is indeed the case, as the low levels of *Foxp3* transcripts in the cancer cells were derived exclusively from the mutant alleles.

Our analysis of human breast cancer samples provides strong support for an important role for the *FOXP3* gene in the development of breast cancer. First, we searched X-chromosomal deletion using three markers encompassing more than 10 MB of Xp11 and found that *FOXP3* is likely the minimal region of deletion. Second, we revealed a high proportion of somatic mutations in the FOXP3 gene (23 of 65 cases over about 2000 bp exon and intron sequence scanned). The significance of our finding can be discerned indirectly based on the fact that the mutations tended to cluster around important domains, such as the forkhead and the zinc finger domains. In addition, most of the mutations resulted in the nonconservative replacement of amino acids, and cancers with mutations identified had higher levels of HER-2 than those without mutations. The rate of missense to synonymous mutation was 18/3, which greatly exceeds what would be predicted if the mutations were not relevant to tumor development. More importantly, we demonstrated that two tested mutations in the FKH and zing finger domains inactivated the repressor activity and tumor growth inhibition and that cancer tissues bearing an intronic mutation had an inactive *FOXP3* locus. Moreover, mutations and deletions of the *FOXP3* locus corresponded to increased HER-2 levels. Third, we have documented extensive downregulation of FOXP3 among more than 600 cases of breast cancer tissues.

Foxp3 Is a Major Transcriptional Repressor for *ErbB2*

The molecular lesions leading to HER-2 overexpression remain poorly understood. Here we showed that the *Foxp3* mutation resulted in overexpression of *ErbB2*, the murine homolog of *HER-2*. In addition, transfection of *Foxp3* repressed *ErbB2* transcription. More importantly, chromatin immunoprecipitation and EMSA analyses revealed that Foxp3 binds specifically to its consensus sequence in the 5′ of the *ErbB2* gene. Since specific mutations in the promoter abrogate its susceptibility to repression by Foxp3, such binding is likely responsible for it.

Importantly, we have demonstrated that for TSA cell line, which has ErbB2 overexpression, repressing the *ErbB2* locus is responsible for Foxp3's tumor suppressor activity. The requirement for continuous expression of *ErbB2* is best explained by the concept of oncogene addiction (Weinstein, 2002). However, FOXP3 can also suppress the growth of tumor cell lines that do not grossly overexpress *HER-2/ErbB2*, such as MCF-7. In an effort to identify other potential FOXP3 targets, we have produced a FOXP3-Tet-off MCF-7 cell line that expresses FOXP3 upon removal of tetracycline (Figure S5A). Using the most current version of Entrez gene-based CDFs for a more accurate GeneChip analysis (Dai et al., 2005), we uncovered widespread changes in the expression of genes that are involved in several pathways critical for cancer cell growth (Figure S5B). Interestingly, ten genes involved in ErbB2 signaling pathway were repressed by FOXP3 (Figure S5C). Thus, multiple oncogenes can potentially be upregulated by *FOXP3* inactivation. Taken together, we have demonstrated that *FOXP3* is the first X-linked breast cancer suppressor that represses the *HER-2/ErbB2* oncogene. Given the significant role of HER-2 in the pathogenesis of human breast cancer and the widespread defects of the *FOXP3* locus, it is likely that *FOXP3* is an important suppressor for human breast cancer.

EXPERIMENTAL PROCEDURES

Quantitative Real-Time PCR

Relative quantities of mRNA expression were analyzed using real-time PCR (Applied Biosystems ABI Prism 7700 Sequence Detection System, Applied Biosystems). The SYBR (Qiagen) green fluorescence dye was used in this study. The primer sequences (5′-3′) are listed in Table S6.

Chromatin Immunoprecipitation

Chromatin Immunoprecipitation was carried out according to published procedure (Im et al., 2004). Briefly, the Foxp3-V5-transfected TSA cells were sonicated and fixed with 1% paraformaldehyde. The anti-V5 antibodies or control mouse IgG were used to pull down chromatin associated with Foxp3-V5. The amounts of the specific DNA fragment were quantitated by real-time PCR and normalized against the genomic DNA preparation from the same cells.

FOXP3-Silencing Lentiviral Vector

The lentivirus-based siRNA expressing vectors were created by introducing the murine U6 RNA polymerase III promoter and a murine phosphoglycerate kinase promoter (pGK)-driven EGFP expression cassette into a vector of pLenti6/V5-D-TOPO backbone without CMV promoter. A hairpin siRNA sequence of *FOXP3* (target sequence at the region of 1256–1274 nucleotides; 5′-GCAGCGGACACTCAAT GAG-3′) was cloned into the lentiviral siRNA expressing vectors by restriction sites of *Apa*I and *Eco*RI.

Immunohistochemistry and Fluorescence In Situ Hybridization (FISH)

HER-2 expression was performed using Pathway HER-2 (Clone CB11) (Ventana Medical Systems, Inc., Tucson, AZ) on the BenchMark XT automated system per the manufacturer's recommended protocol. The HER-2 levels were scored by commonly used criteria (Yaziji et al., 2004).

FISH for FOXP3 deletion was done using BAC clone RP11-344O14 (ntLocus X: 48,817,975–48,968,223), which was verified by PCR to contain the FOXP3 gene. The minimal common region of deletion was done using flanking p-telomeric and centromeric clones, RP11-573N21 (ntLocus X: 43,910,391–44,078,600) and RP11-353K22 (ntLocus X: 54,416,890–54,545,788), respectively.

EMSA

Nuclear extracts were prepared as described previously (Wang et al., 1999). The sequence for the WT probe (W) was AGTTCAATTTG AATTTCAGATAAACG. Mutant probe (M) (AGTTCAGCGCGAGCGC CAGAGCGCCG) with mutations of all three potential forkhead binding sites was used as specificity control.

Supplemental Data

Supplemental Data include six tables, five figures, Supplemental Experimental Procedures, and Supplemental References and can be found with this article online at http://www.cell.com/cgi/content/full/129/7/1275/DC1/.

ACKNOWLEDGMENTS

We thank Dr. Fan Meng for assistance in bioinformatics, Drs. Eric Fearon, Albert de la Chapelle, Zhaohui Qin, Michael Caligiuri, and Charis Eng for their valuable discussions and/or critical reading of the manuscript, and Lynde Shaw for secretarial assistance. This study is supported by grants from the National Institutes of Health and the Department of Defense.

Received: July 6, 2006
Revised: September 12, 2006
Accepted: April 10, 2007
Published online: June 14, 2007

REFERENCES

Bennett, C.L., Christie, J., Ramsdell, F., Brunkow, M.E., Ferguson, P.J., Whitesell, L., Kelly, T.E., Saulsbury, F.T., Chance, P.F., and Ochs, H.D. (2001). The immune dysregulation, polyendocrinopathy, enteropathy, X-linked syndrome (IPEX) is caused by mutations of FOXP3. Nat. Genet. *27*, 20–21.

Bofin, A.M., Ytterhus, B., Martin, C., O'Leary, J.J., and Hagmar, B.M. (2004). Detection and quantitation of HER-2 gene amplification and protein expression in breast carcinoma. Am. J. Clin. Pathol. *122*, 110–119.

Brunkow, M.E., Jeffery, E.W., Hjerrild, K.A., Paeper, B., Clark, L.B., Yasayko, S.A., Wilkinson, J.E., Galas, D., Ziegler, S.F., and Ramsdell, F. (2001). Disruption of a new forkhead/winged-helix protein, scurfin, results in the fatal lymphoproliferative disorder of the scurfy mouse. Nat. Genet. *27*, 68–73.

Chang, X., Gao, J.X., Jiang, Q., Wen, J., Seifers, N., Su, L., Godfrey, V.L., Zuo, T., Zheng, P., and Liu, Y. (2005). The Scurfy mutation of FoxP3 in the thymus stroma leads to defective thymopoiesis. J. Exp. Med. *202*, 1141–1151.

Chatila, T.A., Blaeser, F., Ho, N., Lederman, H.M., Voulgaropoulos, C., Helms, C., and Bowcock, A.M. (2000). JM2, encoding a fork head-related protein, is mutated in X-linked autoimmunity-allergic disregulation syndrome. J. Clin. Invest. *106*, R75–R81.

Dai, M., Wang, P., Boyd, A.D., Kostov, G., Athey, B., Jones, E.G., Bunney, W.E., Myers, R.M., Speed, T.P., Akil, H., et al. (2005). Evolving gene/transcript definitions significantly alter the interpretation of GeneChip data. Nucleic Acids Res. *33*, e175.

Fontenot, J.D., Gavin, M.A., and Rudensky, A.Y. (2003). Foxp3 programs the development and function of CD4+CD25+ regulatory T cells. Nat. Immunol. *4*, 330–336.

Fontenot, J.D., Rasmussen, J.P., Williams, L.M., Dooley, J.L., Farr, A.G., and Rudensky, A.Y. (2005). Regulatory T cell lineage specification by the forkhead transcription factor foxp3. Immunity *22*, 329–341.

Garcia de Palazzo, I., Klein-Szanto, A., and Weiner, L.M. (1993). Immunohistochemical detection of c-erbB-2 expression by neoplastic human tissue using monospecific and bispecific monoclonal antibodies. Int. J. Biol. Markers *8*, 233–239.

Godfrey, V.L., Wilkinson, J.E., Rinchik, E.M., and Russell, L.B. (1991). Fatal lymphoreticular disease in the scurfy (sf) mouse requires T cells that mature in a sf thymic environment: potential model for thymic education. Proc. Natl. Acad. Sci. USA *88*, 5528–5532.

Godfrey, V.L., Rouse, B.T., and Wilkinson, J.E. (1994). Transplantation of T cell-mediated, lymphoreticular disease from the scurfy (sf) mouse. Am. J. Pathol. *145*, 281–286.

Im, H., Grass, J.A., Johnson, K.D., Boyer, M.E., Wu, J., and Bresnick, E.H. (2004). Measurement of protein-DNA interactions in vivo by chromatin immunoprecipitation. Methods Mol. Biol. *284*, 129–146.

Jimenez, R.E., Wallis, T., Tabasczka, P., and Visscher, D.W. (2000). Determination of Her-2/Neu status in breast carcinoma: comparative analysis of immunohistochemistry and fluorescent in situ hybridization. Mod. Pathol. *13*, 37–45.

Kallioniemi, O.P., Kallioniemi, A., Kurisu, W., Thor, A., Chen, L.C., Smith, H.S., Waldman, F.M., Pinkel, D., and Gray, J.W. (1992). ERBB2 amplification in breast cancer analyzed by fluorescence in situ hybridization. Proc. Natl. Acad. Sci. USA *89*, 5321–5325.

Knudson, A.G., Jr. (1971). Mutation and cancer: statistical study of retinoblastoma. Proc. Natl. Acad. Sci. USA *68*, 820–823.

Kristiansen, M., Knudsen, G.P., Maguire, P., Margolin, S., Pedersen, J., Lindblom, A., and Orstavik, K.H. (2005). High incidence of skewed X chromosome inactivation in young patients with familial non-BRCA1/BRCA2 breast cancer. J. Med. Genet. *42*, 877–880.

Miki, Y., Swensen, J., Shattuck-Eidens, D., Futreal, P.A., Harshman, K., Tavtigian, S., Liu, Q., Cochran, C., Bennett, L.M., Ding, W., et al. (1994). A strong candidate for the breast and ovarian cancer susceptibility gene BRCA1. Science *266*, 66–71.

Piao, Z., and Malkhosyan, S.R. (2002). Frequent loss Xq25 on the inactive X chromosome in primary breast carcinomas is associated with tumor grade and axillary lymph node metastasis. Genes Chromosomes Cancer *33*, 262–269.

Richardson, A.L., Wang, Z.C., De Nicolo, A., Lu, X., Brown, M., Miron, A., Liao, X., Iglehart, J.D., Livingston, D.M., and Ganesan, S. (2006). X chromosomal abnormalities in basal-like human breast cancer. Cancer Cell *9*, 121–132.

Romanov, S.R., Kozakiewicz, B.K., Holst, C.R., Stampfer, M.R., Haupt, L.M., and Tlsty, T.D. (2001). Normal human mammary epithelial cells spontaneously escape senescence and acquire genomic changes. Nature *409*, 633–637.

Roncuzzi, L., Brognara, I., Cocchi, S., Zoli, W., and Gasperi-Campani, A. (2002). Loss of heterozygosity at pseudoautosomal regions in human breast cancer and association with negative hormonal phenotype. Cancer Genet. Cytogenet. *135*, 173–176.

Samuels, Y., Wang, Z., Bardelli, A., Silliman, N., Ptak, J., Szabo, S., Yan, H., Gazdar, A., Powell, S.M., Riggins, G.J., et al. (2004). High frequency of mutations of the PIK3CA gene in human cancers. Science *304*, 554.

Schechter, A.L., Stern, D.F., Vaidyanathan, L., Decker, S.J., Drebin, J.A., Greene, M.I., and Weinberg, R.A. (1984). The neu oncogene: an erb-B-related gene encoding a 185,000-Mr tumour antigen. Nature *312*, 513–516.

Slamon, D.J., Clark, G.M., Wong, S.G., Levin, W.J., Ullrich, A., and McGuire, W.L. (1987). Human breast cancer: correlation of relapse and survival with amplification of the HER-2/neu oncogene. Science *235*, 177–182.

Slamon, D.J., Leyland-Jones, B., Shak, S., Fuchs, H., Paton, V., Bajamonde, A., Fleming, T., Eiermann, W., Wolter, J., Pegram, M., et al. (2001). Use of chemotherapy plus a monoclonal antibody against HER2 for metastatic breast cancer that overexpresses HER2. N. Engl. J. Med. *344*, 783–792.

Spatz, A., Borg, C., and Feunteun, J. (2004). X-Chromosome genetics and human cancer. Nat. Rev. Cancer *4*, 617–629.

Todorovic-Rakovic, N., Jovanovic, D., Neskovic-Konstantinovic, Z., and Nikolic-Vukosavljevic, D. (2005). Comparison between immunohistochemistry and chromogenic in situ hybridization in assessing HER-2 status in breast cancer. Pathol. Int. *55*, 318–323.

Wang, C.Y., Cusack, J.C., Jr., Liu, R., and Baldwin, A.S., Jr. (1999). Control of inducible chemoresistance: enhanced anti-tumor therapy through increased apoptosis by inhibition of NF-kappaB. Nat. Med. *5*, 412–417.

Weinstein, I.B. (2002). Cancer. Addiction to oncogenes–the Achilles heal of cancer. Science *297*, 63–64.

Wildin, R.S., Ramsdell, F., Peake, J., Faravelli, F., Casanova, J.L., Buist, N., Levy-Lahad, E., Mazzella, M., Goulet, O., Perroni, L., et al. (2001). X-linked neonatal diabetes mellitus, enteropathy and endocrinopathy syndrome is the human equivalent of mouse scurfy. Nat. Genet. *27*, 18–20.

Wooster, R., Bignell, G., Lancaster, J., Swift, S., Seal, S., Mangion, J., Collins, N., Gregory, S., Gumbs, C., and Micklem, G. (1995). Identification of the breast cancer susceptibility gene BRCA2. Nature *378*, 789–792.

Wooster, R., and Weber, B.L. (2003). Breast and ovarian cancer. N. Engl. J. Med. *348*, 2339–2347.

Xing, X., Wang, S.C., Xia, W., Zou, Y., Shao, R., Kwong, K.Y., Yu, Z., Zhang, S., Miller, S., Huang, L., and Hung, M.C. (2000). The ets protein PEA3 suppresses HER-2/neu overexpression and inhibits tumorigenesis. Nat. Med. *6*, 189–195.

Yaziji, H., Goldstein, L.C., Barry, T.S., Werling, R., Hwang, H., Ellis, G.K., Gralow, J.R., Livingston, R.B., and Gown, A.M. (2004). HER-2 testing in breast cancer using parallel tissue-based methods. JAMA *291*, 1972–1977.

Ziegler, S.F. (2006). FOXP3: Of mice and men. Annu. Rev. Immunol. *24*, 209–226.